ChemComm



COMMUNICATION

View Article Online



Cite this: DOI: 10.1039/c5cc08630b

Received 17th October 2015, Accepted 8th December 2015

DOI: 10.1039/c5cc08630b

www.rsc.org/chemcomm

Anion-induced palladium nanoparticle formation during the on-surface growth of molecular assemblies†

Michael Morozov,^a Tatyana Bendikov,^b Guennadi Evmenenko,^c Pulak Dutta,^c Michal Lahav^a and Milko E. van der Boom*^a

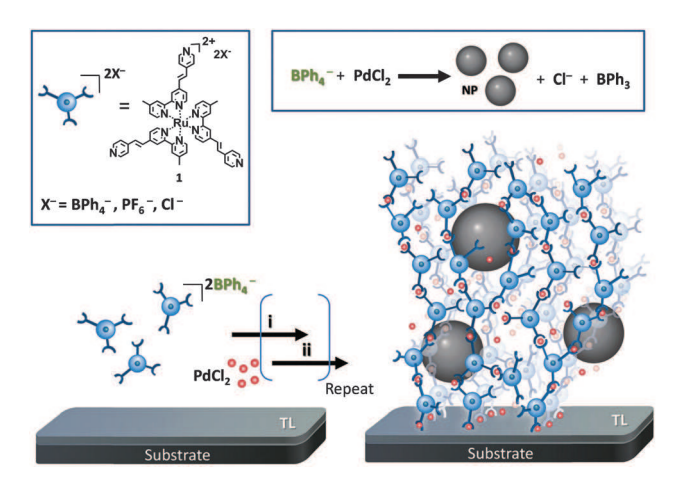
We demonstrate a process that results in the formation of palladium nanoparticles during the assembly of molecular thin films. These nanoparticles are embedded in the films and are generated by a chemical reaction of the counter anions of the molecular components with the metal salt that is used for cross-linking these components.

Anions are known to control the structures and functions of complex and large coordination-based structures including molecular cages. The importance of the role that anions play in numerous supramolecular processes cannot be overstated. In most cases, the anions play a structure stabilizing role and do not undergo chemical transformations.

The stepwise assembly of coordination-based polymers from solution on solid interfaces has opened up many possibilities for systematically studying and controlling their properties.⁵⁻⁷ These materials are being studied for their properties in relation to electron transfer, 8-12 electrochromics, 12-15 solar cells, 16 and Boolean logic. 17,18 Nishihara and others have reported structural factors that affect the electrochemical and the electron transport properties of surface-bound metallo-organic oligomers.8-12,19-21 The formation of such materials often includes the build-up of metal complexes during the assembly procedure, 22-24 or the use of structurally defined complexes that are being integrated into larger structures.²² We have reported that the alternative deposition of polypyridyl complexes of cobalt, iron, ruthenium, osmium, as well as palladium dichloride from solution results in linear and exponentially growing molecular assemblies. 25,26 The overall reaction is essentially a three-component process in which the self-propagating molecular assemblies (SPMAs) store

We introduce here an assembly process that generates coordination-based molecular materials with the concurrent formation of embedded metallic nanoparticles. This new process is demonstrated by the formation of composite materials consisting of redox-active ruthenium complexes ($1 \cdot BPh_4$) and palladium nanoparticles (PdNPs) (Scheme 1). Pre-synthesized NPs have been embedded in thin films from solution using Layer-by-Layer (LbL) deposition and other methods. The methods are duction process has been used as well. In our method, PdNPs are generated *in situ* by a redox reaction between the tetraphenylborate anions (BPh $_4$) of the ruthenium complexes and an excess of palladium($_1$) present in the films. Tetraphenylborate is known to reduce palladium($_1$).

The new PdNP-containing SPMAs were formed by using a stepwise assembly procedure. Quartz, silicon, and indium-tin-oxide



Scheme 1 Schematic representation of the formation of self-propagating molecular assemblies (SPMAs) by alternating deposition of a Pd salt and complex 1 upon a pyridine-terminated template layer (TL) (Fig. S1 and S2, ESI \dagger). The formal of the anion reduces the Pd(II) to form nanoparticles.

excess of the d^8 palladium salt. The palladium salt is used to coordinatively bind polypyridyl complexes from solution to the surface of the assembly.²⁵

^a Department of Organic Chemistry, Weizmann Institute of Science, Rehovot 7610001, Israel. E-mail: milko.vanderboom@weizmann.ac.il

b Department of Chemical Research Support, Weizmann Institute of Science, Rehovot 7610001. Israel

^cDepartment of Physics and Astronomy and Department of Materials Science and Engineering, Northwestern University, Evanston, Illinois 60208, USA

[†] Electronic supplementary information (ESI) available: Experimental procedures and characterization data. See DOI: 10.1039/c5cc08630b

(ITO)-coated glass substrates were functionalized with a template layer (TL)³⁴ having pyridine groups available for coordination to palladium (Fig. S2, ESI†). Subsequently, twelve iterative 15 min immersions of these substrates into a THF solution of $PdCl_2(PhCN)_2$ (1.0 mM) and a THF/DMF (3:7 v/v; 0.2 mM) solution of complex 1·BPh₄ resulted in the formation of the SPMAs. The films were washed and sonicated (3 \times 3 min) in organic solvents between the deposition steps. The SPMAs have been characterized by combining several complementary analytical methods: optical (UV/Vis and ellipsometry) spectroscopy, synchrotron X-ray reflectivity (XRR), X-ray photoelectron spectroscopy (XPS), scanning electron microscopy (SEM), atomic force microscopy (AFM) and electrochemistry. For comparison, we also

generated an SPMA with complex 1-PF₆.

Communication

The UV/Vis measurements indicated a near-linear growth for 1.BPh₄ and exponential growth for 1.PF₆. For both SPMAs, a good correlation was observed between the number of depositions of the polypyridyl complexes, and the intensity of the ligand $\pi \to \pi^*$ and the metal-to-ligand-charge transfer (MLCT) absorption bands at $\lambda = 316$ nm and $\lambda = 500$ nm, respectively (Fig. 1A and Fig. S3, ESI \dagger). The noticeable difference (3×) in the increase in the optical absorption for 1·BPh₄ and 1·PF₆ (Fig. 1A, inset) can be attributed to the reduction of Pd(II) by BPh₄⁻ and the subsequent formation of NPs (vide infra). Therefore, less PdCl₂ is available for binding of additional complexes of 1·BPh₄ to the assembly resulting in near-linear growth. The linear versus exponential growth for SPMAs is a function of the available metal salt. 25,26 The film thicknesses obtained by ellipsometry also showed near-linear growth for 1-BPh4 and exponential growth for 1.PF₆ (Fig. 1B). The linear dependence between the absorption intensities and the thicknesses indicates that the structural regularity was maintained during the growth (Fig. S9, ESI†). The molecular densities for both SPMAs are very similar: 0.8 molecules per nm³ (1·BPh₄) and 1.0 molecules per nm³ (1·PF₆). We also build-up an SPMA by twelve alternating depositions of 1·BPh4 and 1·PF6, starting with the deposition of 1.PF6. Interestingly, the UV/Vis and ellipsometry data show that the growth of this SPMA follows the same trend observed for the SPMA formed from 1.PF₆ (Fig. S4, ESI†). Apparently, the presence of 1-PF₆ in each alternating layer is

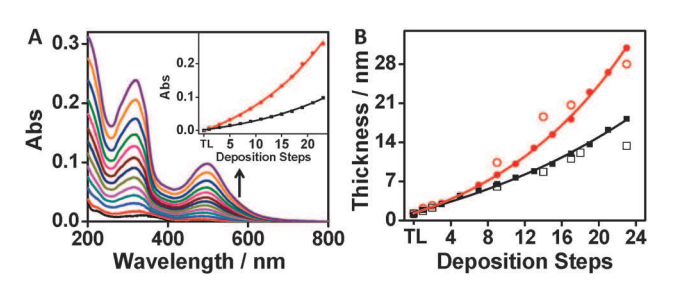


Fig. 1 (A) UV/Vis absorption data of self-propagating molecular assemblies (SPMAs) for 12 depositions of $\bf 1.BPh_4$. Inset: Absorption intensities of the MLCT band (λ = 500 nm) versus the number of $\bf 1.BPh_4$ (black) or $\bf 1.PF_6$ (red) deposition steps. (B) SPMA thickness versus the number of $\bf 1.BPh_4$ (black) or $\bf 1.PF_6$ (red) deposition steps. Closed symbols = ellipsometry and open symbols = X-ray reflectivity. $R^2 \geq 0.998$ for all fits. TL refers to the template layer (Fig. S2, ESI†). 34

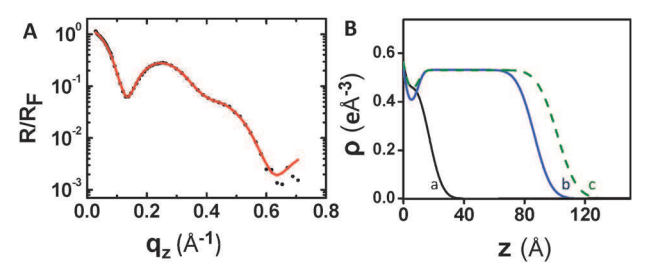
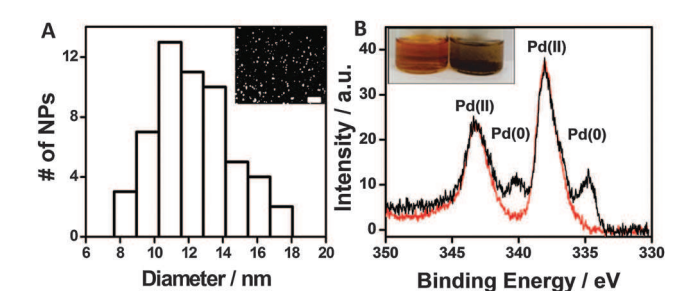


Fig. 2 (A) Representative synchrotron X-ray reflectivity (XRR) data: self-propagating molecular assemblies (SPMAs) formed from $\mathbf{1} \cdot \mathbf{BPh_4}$ (6.1 nm; roughness 8.4 Å) on a silicon substrate in which R is the reflectivity normalized to the Fresnel reflectivity $R_{\rm F}$. The red trace is a fit to the experimental data.³⁵ (B) XRR-derived electron density profiles for the template layer (TL; solid line a; Fig. S2, ESI†), SPMAs formed from $\mathbf{1} \cdot \mathbf{BPh_4}$ [solid line, b (8.7 nm)] and from $\mathbf{1} \cdot \mathbf{PF_6}$ [dashed line, c (10.5 nm)]. The minima at around 0.8 nm represent the TL (a)³⁴ and the plateaus correlate to the SPMAs.

sufficient to maximize the film growth. A similar observation has been reported when using layers of two different molecular building blocks in one assembly.³⁴ The layers consisting of polypyridyl complexes induced exponential growth in layers of organic chromophores.

Selected samples of SPMAs, generated from $1 \cdot \text{BPh}_4$ or $1 \cdot \text{PF}_6$, were analyzed by synchrotron XRR measurements (XRRs), ³⁵ confirming the film thicknesses observed by ellipsometry (Fig. 1B and 2, Fig. S5, ESI†). Interestingly, the electron density and roughness ($\rho = 0.53 \text{ e Å}^{-3}$; $R \approx 9 \text{ Å}$) are similar for both SPMAs and remained constant throughout their formation (Fig. 2), thus indicating homogeneous structures. A dendritic divergent growth is unlikely to exhibit such an electron density profile. ³⁶ AFM measurements of SPMAs having a thickness of 12 nm indicated that they share similar surface morphologies with $R_{\rm rms} \approx 0.5$ nm, and exhibit areas having depths of 1.5–3.0 nm and widths of 10–35 nm.

SEM analysis of those SPMAs having a thickness of 12 nm revealed the formation of NPs only with 1.BPh4. These NPs have an average diameter of \sim 12.5 nm (Fig. 3A). High-resolution XPS spectra acquisition revealed the presence of significant amounts (20%) of Pd(0) in the SPMAs generated with $1{\cdot}BPh_4$ (Fig. 3B); $E_{\rm B}({\rm Pd}_{5/2}~\approx~335~{\rm eV}).^{37}$ Metal centers are known to undergo reduction during the measurements; however, the amount of Pd(0) remained constant during the measurements. Therefore, the observed Pd(0) is the result of a reduction reaction with the surface-bound 1.BPh4 and PdCl2(PhCN)2. These findings are in good agreement with the SEM data and the expected reactivity of 1.BPh4 and 1.PF6 with the palladium salt. Although similar amounts of excess Pd(II) are observed by XPS for both SPMAs [Pd/Ru \approx 3 at 0 $^{\circ}$ takeoff angle; $E_{\rm B}({\rm Pd}_{5/2} \approx 338 \ {\rm eV})]^{37}$ the growth with ${\bf 1} \cdot {\bf BPh_4}$ is less efficient, which may be explained by the trapping of some of the Pd(II) by the NPs. The theoretical Pd/Ru ratio is 1.5 for a saturated network with all the vinylpyridines of 1.BPh4 or 1.PF6 cross-linked with palladium. To confirm the reactivity of BPh₄⁻ with PdCl₂, both model complexes Ru(bpy)₃(PF₆)₂ and Ru(bpy)₃(BPh₄)₂ were reacted with PdCl2(PhCN)2 in solution to evaluate their reactivity and structural stability. Mixing Ru(bpy)₃(BPh₄)₂ with PdCl₂(PhCN)₂



ChemComm

Fig. 3 (A) The size distribution of palladium NPs of self-propagating molecular assemblies (SPMAs) formed from 1·BPh₄ (12 nm). Inset: scanning electron microscopy (SEM) image. The white scale bar = 100 nm. (B) Normalized X-ray photoelectron spectroscopy (XPS) spectra of the Pd 3d region for SPMAs (10 nm) formed from 1-BPh₄ (black line) and from 1-PF₆ (red line). 37 The samples were measured at a takeoff angle of $0^{\circ}.$ Inset: Photographs showing glass vials of the reaction of PdCl₂(PhCN)₂ with $Ru(bpy)_3(PF_6)_2$ (left) or $Ru(bpy)_3(BPh_4)_2$ (right) (Fig. S6, ESI†). For (A) and (B), silicon substrates were used.

resulted in an electron-transfer, as judged by the formation of colloidal palladium and a change in the solution's color from orange to brown (Fig. 3B inset and Fig. S6, ESI†). The formation of triphenylborane (BPh3) was observed by 11B(1H) NMR, which showed a singlet resonance at δ 45 ppm. 38,39 UV/Vis spectrometry and mass spectrometry indicated that the molecular structure of the Ru(bpy)₃ remained intact with chloride as the counter anion. XPS measurements of the black precipitate revealed the formation of Pd(0). As expected, no reduction of Pd(II) was observed when $Ru(bpy)_3(PF_6)_2$ was used.

Cyclic voltammetry measurements showed that SPMAs with thicknesses of 7 nm and 12 nm exhibit well-defined surface wave characteristic of the Ru^{2+/3+} couple on ITO with a half-wave redox potential, $E_{1/2}$, at about 1.2 V versus Ag/Ag⁺ (with ferrocene as an internal reference, $E_{1/2} = 0.40 \text{ V}$) (Fig. 4A and Fig. S7, ESI†). The $E_{1/2}$ value was not affected by the differences in thickness and the presence of the palladium NPs. The permeability of the two SPMAs (7 nm thickness) was evaluated using two electrochemically active probes having different volumes (estimated by DFT): 2,6-dimethoxy-1,4-benzoquinone (228 Å^3) and 3,3',5,5'tetra-tertbutyldiphenylphenoquinone (640 Å³) (Fig. 4B and Fig. S8, ESI†). The SPMA generated with 1.BPh4 is slightly more porous than the SPMA formed from 1.PF6 as indicated by the difference in the anodic and cathodic peak currents, i_{pa} and i_{pc} . Our observations are in good agreement with our previous mechanistic studies showing that the SPMAs are porous structures capable of storing and using metal salts for their growth. $\!\!^{25,26,35,40}$

The counter anions of cationic metal complexes can be used to generate composite assemblies by redox chemistry. The deposition steps in the here-presented assembly do not just add materials to the surface; they enforce multiple transformations including the formation of nanoparticles. Overall, the structure and properties of such assemblies, consisting of both molecular components and metallic NPs, very much resemble those of assemblies lacking the NPs. However, less material is being deposited for the NP containing assembly. Besides the presence of the NPs, large structural differences between the supramolecular

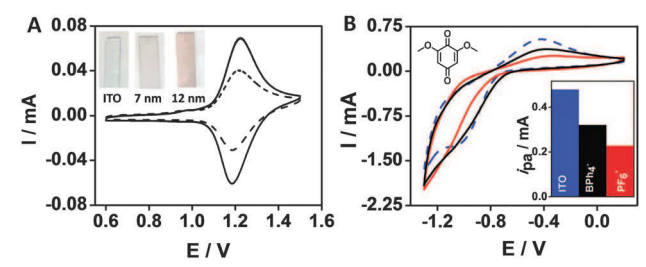


Fig. 4 (A) Representative cyclic voltammograms (CVs) of self-propagating molecular assemblies (SPMAs) formed from **1 BPh₄** (7 nm, dotted line; 12 nm, solid line) recorded on a single-sided ITO-coated glass. Inset: Photographs of the electrodes (0.7 cm \times 2 cm). (B) Representative CVs of 2,6-dimethoxy-1,4-benzoquinone (1.3 mM, CH₃CN) for a double-sided ITO electrode (blue line), and the same electrodes coated with SPMAs formed from 1·BPh₄ (7 nm, black line) and from 1·PF₆ (7 nm; red line). Inset: Bar diagram showing the differences in the anodic peak currents (i_{pa}) for the three systems. The experiments were carried out at rt under argon in 0.1 M ⁿBu₄NPF₆/CH₃CN at a scan rate of 100 mV s⁻¹. The ITO-coated glass, Pt wire and Ag/Ag⁺ were used as working, counter, and reference electrodes, respectively

structures are not apparent from the optical, XRR and electrochemical data, including the permeability of the assemblies by organic molecules. The molecular density is nearly identical regardless of the presence of metallic NPs. Significant differences were found in the growth of the assemblies; the assemblies with the NPs grow slower. The in situ generation of NPs by and from the different building blocks and their subsequent integration into the assemblies can be considered to be a new route to the formation of functional coatings with a high degree of structural complexity.

This research was supported by the Helen and Martin Kimmel Center for Molecular Design, the Israel Science Foundation (289/09), MINERVA. The use of the Advanced Photon Source was supported by the U.S. Department of Energy, Office of Science, Office of Basic Energy Sciences, under Contract No. DE-AC02-06CH11357. GE and PD were supported by the U.S. National Foundation under Grant No. DMR-1309589. GE gratefully acknowledges support from the Center for Electrochemical Energy Science (CEES), an Energy Frontier Research Center (EFRC) funded by the U.S. Department of Energy, Office of Science, Office of Basic Energy Sciences (Contract No. DE-AC02-06CH11357). The scanning electron microscopy studies were conducted at the Irving and Cherna Moskowitz Center for Nano and Bio-Nano Imaging at the Weizmann Institute of Science.

Notes and references

- 1 R. Custelcean, Chem. Soc. Rev., 2014, 43, 1813-1824.
- 2 M. W. Hosseini and J.-M. Lehn, Helv. Chim. Acta, 1986, 69, 587-603.
- 3 L. J. Kaplan, G. R. Weisman and D. J. Cram, J. Org. Chem., 1979, 44, 2226-2233.
- 4 I. A. Riddell, M. M. J. Smulders, J. K. Clegg, Y. R. Hristova, B. Breiner, J. D. Thoburn and J. R. Nitschke, Nat. Chem., 2012, 4, 751-756.
- 5 I. Rubinstein and A. Vaskevich, Isr. J. Chem., 2010, 50, 333-346.
- 6 H. E. Katz, *Chem. Mater.*, 1994, 6, 2227–2232. 7 D. Zacher, R. Schmid, C. Wöll and R. A. Fischer, *Angew. Chem., Int.* Ed., 2011, 50, 176-199.
- 8 R. Balgley, S. Shankar, M. Lahav and M. E. van der Boom, Angew. Chem., Int. Ed., 2015, 54, 12457-12462.

Communication ChemComm

- 9 Y. Nishimori, K. Kanaizuka, T. Kurita, T. Nagatsu, Y. Segawa, F. Toshimitsu, S. Muratsugu, M. Utsuno, S. Kume, M. Murata and H. Nishihara, Chem. - Asian J., 2009, 4, 1361-1367.
- 10 N. Tuccitto, V. Ferri, M. Cavazzini, S. Quici, G. Zhavnerko, A. Licciardello and M. A. Rampi, Nat. Mater., 2009, 8, 41-46.
- J. Liu, T. Wächter, A. Irmler, P. G. Weidler, H. Gliemann, F. Pauly, V. Mugnaini, M. Zharnikov and C. Wöll, ACS Appl. Mater. Interfaces, 2015, 7, 9824-9830.
- L. Motiei, M. Lahav, A. Gulino, M. A. Iron and M. E. van der Boom, J. Phys. Chem. B, 2010, 114, 14283-14286.
- 13 S. Shankar, M. Lahav and M. E. van der Boom, J. Am. Chem. Soc., 2015, 137, 4050-4053.
- M. Schott, W. Szczerba and D. G. Kurth, Langmuir, 2014, 30, 10721-10727.
- 15 K. Takada, R. Sakamoto, S.-T. Yi, S. Katagiri, T. Kambe and H. Nishihara, *J. Am. Chem. Soc.*, 2015, 137, 4681–4689.
 16 L. Motiei, Y. Yao, J. Choudhury, H. Yan, T. J. Marks, M. E. van der
- Boom and A. Facchetti, J. Am. Chem. Soc., 2010, 132, 12528-12530.
- P. C. Mondal, V. Singh, Y. L. Jeyachandran and M. Zharnikov, ACS Appl. Mater. Interfaces, 2015, 7, 8677-8686.
- G. de Ruiter and M. E. van der Boom, Acc. Chem. Res., 2011, 44, 563-573.
- 19 V. Kaliginedi, H. Ozawa, A. Kuzume, S. Maharajan, I. V. Pobelov, N. H. Kwon, M. Mohos, P. Broekmann, K. M. Fromm, M.-A. Haga and T. Wandlowski, Nanoscale, 2015, 7, 17685-17692.
- X. Li, X. Zhao, J. Zhang and Y. Zhao, Chem. Commun., 2013, 49, 10004-10006.
- G. de Ruiter, M. Lahav and M. E. van der Boom, Acc. Chem. Res., 2014, 47, 3407-3416.
- Y. Liang and R. H. Schmehl, J. Chem. Soc., Chem. Commun., 1995,
- T. Heinrich, C. H.-H. Traulsen, M. Holzweber, S. Richter, V. Kunz, S. K. Kastner, S. O. Krabbenborg, J. Huskens, W. E. S. Unger and C. A. Schalley, J. Am. Chem. Soc., 2015, 137, 4382-4390.

- 24 J. Poppenberg, S. Richter, C. H. H. Traulsen, E. Darlatt, B. Baytekin, T. Heinrich, P. M. Deutinger, K. Huth, W. E. S. Unger and C. A. Schalley, Chem. Sci., 2013, 4, 3131-3139.
- 25 J. Choudhury, R. Kaminker, L. Motiei, G. d. Ruiter, M. Morozov, F. Lupo, A. Gulino and M. E. van der Boom, J. Am. Chem. Soc., 2010, 132, 9295-9297.
- 26 L. Motiei, M. Feller, G. Evmenenko, P. Dutta and M. E. van der Boom, Chem. Sci., 2012, 3, 66-71.
- T. Shirman, R. Kaminker, D. Freeman and M. E. van der Boom, ACS Nano, 2011, 5, 6553-6563.
- 28 A. A. Mamedov and N. A. Kotov, *Langmuir*, 2000, **16**, 5530–5533. 29 S. Kinge, M. Crego-Calama and D. N. Reinhoudt, *ChemPhysChem*, 2008, 9, 20-42.
- 30 S. Prakash, T. Chakrabarty, A. K. Singh and V. K. Shahi, Biosens. Bioelectron., 2013, 41, 43-53.
- 31 A. N. Shipway and I. Willner, *Chem. Commun.*, 2001, 2035–2045. 32 C. H.-H. Traulsen, V. Kunz, T. Heinrich, S. Richter, M. Holzweber, A. Schulz, L. K. S. von Krbek, U. T. J. Scheuschner, J. Poppenberg, W. E. S. Unger and C. A. Schalley, Langmuir, 2013, 29, 14284-14292.
- 33 C. Sik Cho, K. Itotani and S. Uemura, J. Organomet. Chem., 1993, 443, 253-259.
- 34 L. Motiei, M. Sassi, R. Kaminker, G. Evmenenko, P. Dutta, M. A. Iron and M. E. van der Boom, Langmuir, 2011, 27, 1319-1325.
- 35 G. Evmenenko, M. E. van der Boom, J. Kmetko, S. W. Dugan, T. J. Marks and P. Dutta, J. Chem. Phys., 2001, 115, 6722-6727.
- 36 T. Shinomiya, H. Ozawa, Y. Mutoh and M. Haga, Dalton Trans., 2013, 42, 16166-16175.
- 37 A. V. Naumkin, A. Kraut-Vass, S. W. Gaarenstroom and C. J. Powell, NIST Standard Reference Database 20, Version 4.1., 2012.
- 38 H. C. Brown and U. S. Racherla, Tetrahedron Lett., 1985, 26, 4311-4314.
- 39 M. R. Hansen, T. Vosegaard, H. J. Jakobsen and J. Skibsted, J. Phys. Chem. A, 2004, 108, 586-594.
- 40 L. Motiei, R. Kaminker, M. Sassi and M. E. van der Boom, J. Am. Chem. Soc., 2011, 133, 14264-14266.